Original article

JOURNAL OF REINFORCED PLASTICS & COMPOSITES

Journal of Reinforced Plastics and Composites
2018, Vol. 37(21) 1304–1321

DOI: 10.1177/0731684418791231
journals.sagepub.com/home/jrp
SAGE

On the estimation and optimization capabilities of the fatigue life prediction models in composite laminates

H Arda Deveci[1,2] and H Seçil Artem[1]

Abstract

In this study, the estimation and optimization capabilities of the multiaxial fatigue life prediction models, namely, Failure Tensor Polynomial in Fatigue, Fawaz–Ellyin, Sims–Brogdon and Shokrieh–Taheri are investigated comparatively. Fatigue life predictions are obtained for multidirectional graphite/epoxy, glass/epoxy, carbon/epoxy and carbon/PEEK composite laminate data taken from the literature. The prediction study shows that the models can predict the fatigue behavior of the multidirectional laminates at different degrees of proximity. In the optimization, a hybrid algorithm combining particle swarm algorithm and generalized pattern search algorithm is used to search the optimum stacking sequence designs of the laminated composites for maximum fatigue life. The hybrid algorithm shows superior performance in terms of computational time and finding improved global optima compared to the best results presented in the literature. After the capability of the models and the reliability of the algorithm are revealed, several lay-up design problems involving different cyclic loading scenarios are solved. The results indicate that the reliability of the optimization may considerably change according to the used model even if the model may yield reasonable prediction results.

Keywords

Composite laminates, multiaxial fatigue, life prediction, optimization, hybrid algorithm

Introduction

The use of fiber-reinforced composites has increasingly started being the main driving force in industries such as aerospace, automotive, military and marine automotive due to their advantageous properties like high strength, high stiffness, and low weight. However, as in metallic materials, fatigue damage is an important issue to be considered in composite structures subjected to complex multiaxial stress states during service. Therefore, fatigue requires durability investigation and special lay-up design in the composite structure components that must bear significant cyclic fatigue loads during operation, such as airplanes, wind turbine rotor blades, boats and bridges.[1]

Numerous fatigue theories and methodologies have been developed so far to investigate the fatigue behavior of composite materials and structures. The fatigue life prediction models in the literature can be classified into five categories: empirical, phenomenological modelling; specific damage metrics such as the residual strength and/or stiffness of the examined material; probabilistic; artificial neural network based; and micromechanics. Moreover, the investigation of fatigue behavior of composite structures under multiaxial loadings is more important for the applications subjected to real complex loading conditions as the fatigue damage under uniaxial loading has been clarified in many studies.[2–5] Among these models, only some of them are suitable to address the problem of fatigue life prediction of composite materials under multiaxial stress states. In this respect, it is reported that empirical models which estimate the fatigue life due to constant amplitude loading based on experimental data without making any assumption regarding the

[1]Department of Mechanical Engineering, İzmir Institute of Technology, İzmir, Turkey
[2]Department of Mechanical Engineering, Erzincan Binali Yıldırım University, Erzincan, Turkey

Corresponding author:
H Seçil Artem, Department of Mechanical Engineering, İzmir Institute of Technology, Gülbahçe Kampüsü, Urla 35430, İzmir, Turkey.
Email: secilartem@iyte.edu.tr

micro mechanisms leading to fatigue failure have also practical application potential in fatigue design of composite structures.[1]

Hashin and Rotem[6] presented an empirical fatigue life prediction model based on the different failure modes for unidirectional materials considering the fiber and matrix failure modes independently. The authors then reported that an interlaminar failure mode is encountered when multidirectional composite laminates are considered.[7] Sims and Brogdon[8] proposed a model that modified the Tsai–Hill failure criterion to a fatigue criterion by replacing the static strengths with the corresponding fatigue strengths taking the number of cycles to failure into consideration. This was the first attempt to use a static failure criterion to constitute a fatigue failure criterion. Similarly, Fawaz and Ellyin[9] proposed a multiaxial fatigue life prediction model based on Tsai–Hill static strength failure criterion. The model requires only an experimental S–N curve of a reference off-axis specimen to make estimations. They showed that the model accurately predicts fatigue failure of different unidirectional and bidirectional fiber-reinforced composite materials subjected to uniaxial and multiaxial stresses and different cyclic stress ratios. Philippidis and Vassilopoulos[10] introduced a model which is an extension of the quadratic version of the failure tensor polynomial for the prediction of fatigue life under complex stress states. It is reported that the model yields reliable predictions for both unidirectional and multidirectional laminated composites when compared to experimental data, and can be used in design of composite structures subjected to multiaxial fatigue loadings. Kawai[11] developed a phenomenological fatigue damage mechanics-based model that could take into account the off-axis angle and stress ratio effect under any constant amplitude loading with non-negative mean stresses in order to predict the off-axis fatigue behavior of unidirectional composites. It is shown that the model is capable of adequately predicting the off-axis behavior over a range of non-negative mean stresses. Shokrieh and Taheri-Behrooz[12] developed a model based on strain energy method and Sandhu static failure criterion for predicting fatigue life of unidirectional composite laminates in various fiber orientation angles.

In the optimization point of view, composite materials provide great design possibility by allowing material tailoring to meet preferred design requirements. Fatigue strength is one of the most important requirements to ensure in composite laminate design. This can be possible through an optimum selection of fiber orientations in a laminate. Nevertheless, there are few published studies on the optimum design of laminated composites for maximum fatigue life.[13–17] As the first attempt in this area, Adali[13] introduced a study to obtain the optimum symmetric angle-ply laminate under in-plane tensile fatigue loads for maximum failure load by employing a fatigue failure criterion and determined optimum fiber orientations, thickness ratio and fiber content for constant cyclic lives. Then, Walker[14] proposed a procedure to minimize the thickness of laminated composite plates subjected to cyclic bending loads for specific fatigue lives under a cumulative damage constraint. In these earlier studies on fatigue design optimization, the researchers used fatigue models that were valid only for limited laminate configurations and specific loading conditions. Essentially, more general stacking sequences and loading conditions are supposed to be considered in design optimization for typical applications. In this regard, Ertas and Sonmez[15] showed in their study that the optimum designs of laminated composite plates under in-plane cyclic loading for maximum fatigue life can theoretically be obtained for more general stacking sequences using Fawaz–Ellyin (FWE) model. Muc and Wierzgoń[16] proposed a design methodology to find the optimum stacking sequences having three different fiber orientations for maximum buckling load of composite plates by introducing a new type of discrete design variables. Recently, Deveci and Artem[17] have presented a design methodology to investigate optimum multidirectional stacking sequence design of laminated composites under various in-plane cyclic loads for maximum fatigue life by using another model, failure tensor polynomial in fatigue (FTPF) model.

In the present study, the aforementioned fatigue life prediction models, FTPF, FWE, Sims–Brogdon (SB) and Shokrieh–Taheri (ST) are selected to investigate their prediction capabilities in multidirectional laminates and optimization capabilities in laminate design for maximum fatigue life. In the first part of the study, a comprehensive experimental correlation is performed for different multidirectional composite materials to evaluate the prediction capabilities of the models by comparing each other. In the second part, each model is used to constitute the objective function of its own, and a particle swarm algorithm embedded generalized pattern search algorithm is used as a hybrid algorithm in the optimization. Before the optimization, the effective performance of the proposed hybrid algorithm is shown by comparative results using a test problem with different design cases from the literature. A pre-optimization study is then performed to justify the theoretical derivation procedure to be followed using experimental data from the literature. After these investigations, a number of problems including many design cases are solved for each model separately and the optimum results are presented to discuss.

In the literature, as known, there are many separate studies dealing with the derivation and application of fatigue life prediction models for fiber-reinforced composite laminates. However, except few studies,[1,2,18] the literature is deficient in studies considering the fatigue life prediction models together to make an evaluation about their estimation capabilities on multidirectional laminates. Moreover, few studies[13–17] have conducted on the optimization of composites for fatigue life maximization. In this regard, our study fulfils this gap in the literature and reveals the potential of the selected suitable models for modeling and improvement of fatigue life of laminated composites.

The fatigue life prediction models used in this study are practical to apply to the prediction and optimization procedures in terms of lower cost and time. It is also worth to note at this point that these models do not consider progressive damage and stiffness loss in composite laminates subjected to cyclic fatigue loading.

Fatigue life prediction using different models

The first part of the study includes the determination of fatigue life prediction capability of designated models on multidirectional composite laminates with different materials. Four multiaxial fatigue life prediction models are evaluated for their applicability and predictive ability. These are the models by Philippidis and Vassilopoulos,[10] Fawaz and Ellyin,[9] Sims and Brogdon[8] and Shokrieh and Taheri.[12] The models are selected as they can be easily implemented, and sufficient fatigue test data are available in the literature for evaluation of their accuracy.[1]

Fatigue life prediction models

FTPF model. A modification of the quadratic version of the failure tensor polynomial for the prediction of fatigue strength under complex stress states was introduced by Philippidis and Vassilopoulos[10] and termed as FTPF criterion. The FTPF criterion is based on Tsai-Hahn tensor polynomial[19] and adapted for fatigue.

For a fiber-reinforced composite plate subjected to in-plane loading, Tsai-Hahn tensor polynomial criterion is expressed in the material coordinates by

$$F_{11}\sigma_1^2 + F_{22}\sigma_2^2 + 2F_{12}\sigma_1\sigma_2 + F_1\sigma_1 + F_2\sigma_2 + F_{66}\sigma_6^2 - 1 \leq 0 \tag{1}$$

Here, the components of the failure tensors can be given by

$$F_{11} = \frac{1}{XX'}, \quad F_{22} = \frac{1}{YY'}, \quad F_{66} = \frac{1}{S^2},$$
$$F_1 = \frac{1}{X} - \frac{1}{X'}, \quad F_2 = \frac{1}{Y} - \frac{1}{Y'}, \quad F_{12} = -\frac{1}{2}\sqrt{F_{11}F_{22}} \tag{2}$$

where X and Y represent the failure strengths of the material along the longitudinal and the transverse directions, respectively, and S represents shear failure strength. The prime ($'$) is used for compressive strengths.

For a cyclic in-plane fatigue loading depicted as in Figure 1, the components of failure tensors are functions of the number of cycles N, stress ratio, $R = \sigma_{\min}/\sigma_{\max}$, and the frequency ν, of the loading as

$$F_{ij} = F_{ij}(N, R, \nu), \; F_i = F_i(N, R, \nu), \quad i, j = 1, 2, 6 \tag{3}$$

and the expressions in equation (2) are still valid for the calculation of tensor components but the failure stresses X, X', Y, Y', and S are replaced by the S–N curves of the material along the same directions and under the same conditions. Thus, the failure stresses X, X', Y, Y', S can be expressed as functions of number of cycles, stress ratio and frequency. If the S–N curves of the material are assumed in the general semi-logarithmic form

$$S = A + B\log N \tag{4}$$

then the expressions of the fatigue failure stresses can be written as

$$\begin{aligned} X(N, R, \nu) &= A_X + B_X \log N \\ X'(N, R, \nu) &= A_{X'} + B_{X'} \log N \\ Y(N, R, \nu) &= A_Y + B_Y \log N \\ Y'(N, R, \nu) &= A_{Y'} + B_{Y'} \log N \\ S(N, R, \nu) &= A_S + B_S \log N \end{aligned} \tag{5}$$

It is reported that only $X(N, R, \nu)$, $Y(N, R, \nu)$ and $S(N, R, \nu)$ tensile fatigue failure stresses are sufficient for the FTPF criterion to yield satisfactory predictions. When only these three S–N curves are used, the fatigue failure tensor components can be given by

$$F_{11} = \frac{1}{X^2(N, R, \nu)}, \quad F_{22} = \frac{1}{Y^2(N, R, \nu)},$$
$$F_{66} = \frac{1}{S^2(N, R, \nu)}, \quad F_1 = F_2 = 0 \tag{6}$$

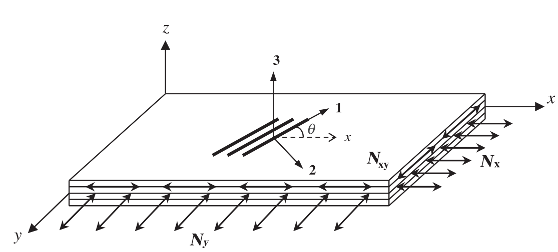

Figure 1. Representative plate geometry showing in-plane loading and principal coordinates.

and by substituting these tensors into equation (1), the criterion finally takes the form

$$\frac{\sigma_1^2}{X^2(N)} + \frac{\sigma_2^2}{Y^2(N)} - \frac{\sigma_1\sigma_2}{X(N)Y(N)} + \frac{\sigma_6^2}{S^2(N)} - 1 \leq 0 \tag{7}$$

where the fatigue failure stresses are shown only as functions of the number of cycles N. The criterion can be used in the form of equation (7) for any stress ratio R, and frequency ν, provided the basic S–N curves are also known for the same R and ν values.

FWE model. Fawaz and Ellyin[9] presented a fatigue life prediction model to simulate the fatigue behavior of unidirectional and multidirectional composite laminates under multiaxial cyclic stress states as presented in Figure 1. The model requires only one experimentally obtained S–N curve and the static strengths of the laminate along different directions. The FWE model assumes that all the on- and off-axis S–N curves of the laminate can be found lying in a narrow band on the S–N plane when they are normalized by the corresponding static strengths.

If a reference S–N curve is expressed by the following semi-log linear relationship

$$S_r = m_r \log(N) + b_r \tag{8}$$

the S–N curve under any off-axis angle can be calculated by

$$S(a_1, a_2, \theta, R, N) = f(a_1, a_2, \theta)\left[g(R)m_r \log(N) + b_r\right] \tag{9}$$

as a function of the reference S–N curve.

In equations (8) and (9), subscript r denotes the reference direction and a_1 and a_2 are the first and second biaxial stress ratios, transverse stress over normal stress (σ_y/σ_x) and shear stress over normal stress (τ_{xy}/σ_x), respectively. m_r and b_r are the parameters derived after fitting to the experimental data of the reference S–N curve. f and g are non-dimensional entities defined by

$$f(a_1, a_2, \theta) = \frac{\sigma_x(a_1, a_2, \theta)}{X_r} \tag{10}$$

$$g(R) = \frac{\sigma_{\max}(1 - R)}{\sigma_{(\max)r} - \sigma_{(\min)r}} \tag{11}$$

where $\sigma_x(a_1, a_2, \theta)$ is the static strength along the longitudinal direction, X_r is the static strength along the reference direction and $\sigma_{(\max)r} - \sigma_{(\min)r}$ is the stress range applied to obtain the reference line.

The off-axis static strengths of the examined material can be estimated using any reliable multiaxial static failure criterion. While defining the model, Fawaz and Ellyin uses Tsai–Hill static failure criterion to determine $\sigma_x(a_1, a_2, \theta)$, thus $f(a_1, a_2, \theta)$. Function g is introduced to take into account different stress ratios, R as seen in equation (11). Note that g is equal to 1 when the stress ratio of the reference S–N curve is the same as that of the S–N curve being predicted $(R = R_r)$, and for $R = 1$ (quasi-static loading), $g = 0$.

Although the FWE criterion has the advantage of requiring only one S–N curve data, the predictions are very sensitive to the selection of the reference curve.

SB model. Sims and Brogdon[8] extended the Tsai–Hill static failure criterion to a fatigue criterion (fatigue life prediction model) by replacing the static strengths with corresponding fatigue functions. The expression of the SB model can be written as

$$\left(\frac{\sigma_1}{\sigma_L}\right)^2 - \frac{\sigma_1\sigma_2}{\sigma_L^2} + \left(\frac{\sigma_2}{\sigma_T}\right)^2 + \left(\frac{\sigma_{12}}{\sigma_S}\right)^2 - 1 \leq 0 \tag{12}$$

where σ_L, σ_T and σ_S denote the fatigue functions (the corresponding S–N curve equations) along the longitudinal, the transverse directions and shear, respectively. σ_1, σ_2 and σ_{12} are the stresses along the material reference system.

The SB model refers to lamina fatigue strength and can be extended to laminates of any orientation using laminated plate theory and knowledge of the stresses in the individual lamina to predict first-ply fatigue failure (the number of cycles). However, the SB model has the same drawback as the Tsai–Hill criterion, which does not take the different strengths of the material under tension and compression into account.

ST model. Shokrieh and Taheri[12] proposed a strain energy-based model for predicting the fatigue life of unidirectional composite laminates at various fiber angles and stress ratios subjected to constant amplitude, tension–tension or compression–compression cyclic loading $(R \geq 0)$. They derived the ST model from the static failure criterion by Sandhu et al.[20] They also adopted the assumption of El Kadi and Ellyin[21] that the relationship between fatigue life and total input energy can be described by the power law type of equation

$$\Delta W^t = kN^{\alpha} + C \tag{13}$$

where k, α and C are material constants. Letting $C = 0$, and k and α are independent of the stress ratio and fiber orientation, the total input energy is defined as

$$\Delta W^{*} = kN^{\alpha} \tag{14}$$

The proposed model in the on-axis coordinate system is given by the following equation

$$\begin{aligned} \Delta W^{*} &= \Delta W_{I}^{*} + \Delta W_{II}^{*} + \Delta W_{III}^{*} \\ &= \frac{\Delta\sigma_1 \Delta\varepsilon_1}{X\varepsilon_{u1}} + \frac{\Delta\sigma_2 \Delta\varepsilon_2}{Y\varepsilon_{u2}} + \frac{\Delta\sigma_6 \Delta\varepsilon_6}{S\varepsilon_{u6}} \end{aligned} \tag{15}$$

where Δ before a symbol indicates its range and ΔW^{*} represents the sum of strain energy densities contributed by all stress components in material directions. ΔW_{I}^{*}, ΔW_{II}^{*} and ΔW_{III}^{*} denote the strain energy densities in the longitudinal, transverse and shear directions, respectively and can be expressed by the set of equations (16)

$$\begin{aligned} \Delta W_{I}^{*} &= \frac{1}{X^2}\frac{(1+R)}{(1-R)}(\Delta\sigma_x)^2(\cos^4\theta) \\ \Delta W_{II}^{*} &= \frac{1}{Y^2}\frac{(1+R)}{(1-R)}(\Delta\sigma_x)^2(\sin^4\theta) \\ \Delta W_{III}^{*} &= \frac{1}{S^2}\frac{(1+R)}{(1-R)}(\Delta\sigma_x)^2(\sin^2\theta\cos^2\theta) \end{aligned} \tag{16}$$

where X, Y and S are the material static strengths; σ_1, σ_2, σ_6, and ε_1, ε_1, ε_6 are stress and strain tensor components; ε_{u1}, ε_{u2} and ε_{u6} are the maximum strains in the principal material directions.

Assuming a linear stress–strain response along the material directions, the conversion of off-axis stresses into the on-axis coordinate (equation (15)) takes the form

$$\Delta W^{*} = \frac{(1+R)}{(1-R)}(\Delta\sigma_x)^2\left(\frac{\cos^4\theta}{X^2} + \frac{\sin^4\theta}{Y^2} + \frac{\sin^2\theta\cos^2\theta}{S^2}\right) \tag{17}$$

where θ is the fiber orientation angle. Equation (17) is valid as long as $R \geq 0$.

The ST model uses both stress and strain to predict failure and only one set of data is required (and used as the reference set) for calibration of the model parameters. However, it seems that the model is only applicable to unidirectional laminates.

Multidirectional laminate predictions for various materials

Prediction capability of the selected models on different composite materials in various multidirectional stacking sequences is investigated by taking multiaxial stress states into consideration. In this respect, a progressive failure approach is adopted to simulate the fatigue behavior of the multidirectional composite laminates. Fatigue life of the laminates is determined by following ply-by-ply analysis. First, for the applied load range of the laminate in question, the stresses in layers are calculated using classical lamination theory, and then fatigue life of the weakest layer is predicted using the related model equation (i.e. equations (7), (9), (12) or (14)) given in a general closed form as

$$f(\sigma_1, \sigma_2, \sigma_6, \log N) - 1 \leq 0 \tag{18}$$

This approach is applied from the first failing ply to the last failing ply by recalculating the stress state on undamaged layers, and thus the final fatigue life of the laminate is determined by the sum of the lives of the layers.

The fatigue life predictions of different multidirectional composite laminates that include graphite/epoxy laminates,[22] carbon/epoxy laminates,[23] E-glass/epoxy laminates,[24] carbon/PEEK laminates[25] are obtained by using the proposed FTPF, SB, FWE and ST models. Predictions of all the models are shown in the same figure for the related laminate configuration to make a comparison of their estimation capabilities. The fatigue life prediction curves are presented with the experimental data (Exp. data) in Figures 2 to 11.

Graphite/epoxy composite laminates. Fatigue life predictions for multidirectional $[0/90]_{4s}$ and $[0/45/-45/90]_{2s}$ graphite/epoxy laminates[22] ($R = -1$) are shown in Figures 2 and 3, respectively. ST model predictions could not be performed since the method restricts the use for negative R values. In the figures, predictions of Ertas and Sonmez[15] obtained by FWE method are also included to give an idea about our prediction performance and reliability. It is noted that the reference

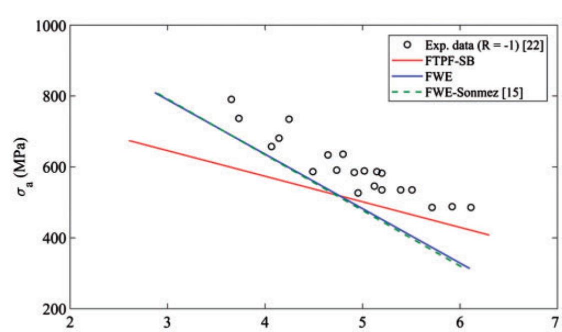

Figure 2. Fatigue life predictions for $[0/90]_{4s}$ graphite/epoxy laminate.

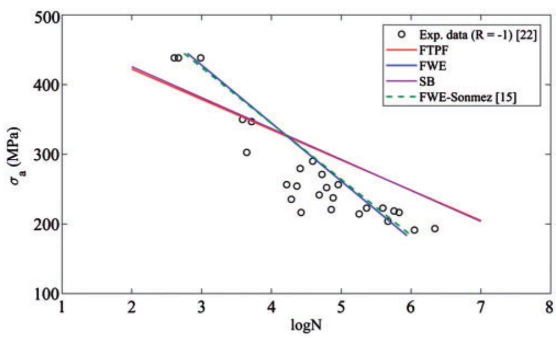

Figure 3. Fatigue life predictions for $[0/45/-45/90]_{2s}$ graphite/epoxy laminate.

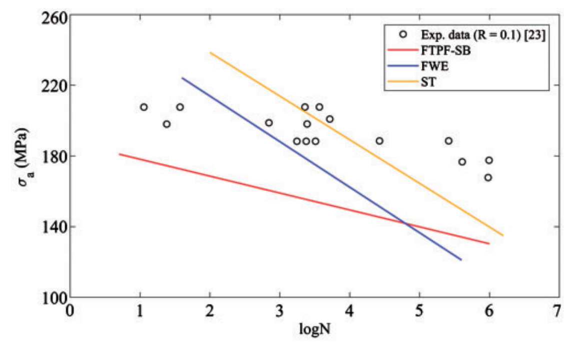

Figure 5. Fatigue life predictions for $[0/90_4]_s$ carbon/epoxy laminate.

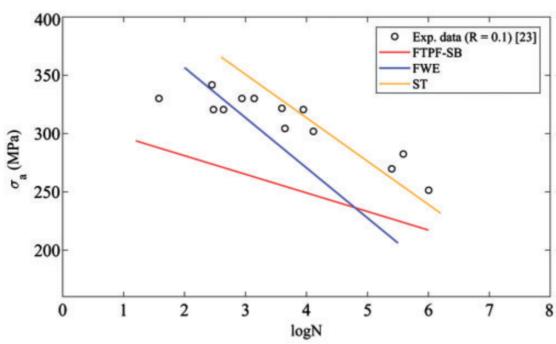

Figure 4. Fatigue life predictions for $[0/90_2]_s$ carbon/epoxy laminate.

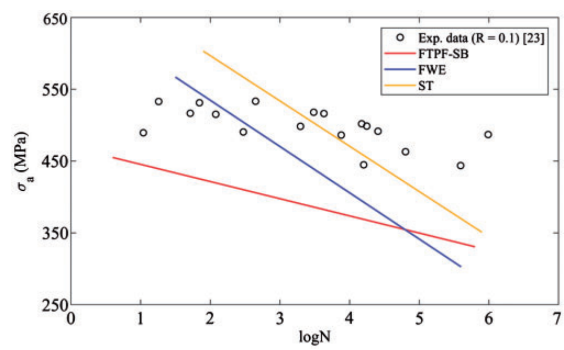

Figure 6. Fatigue life predictions for $[0_2/90_2]_s$ carbon/epoxy laminate.

curve of $[\pm45]_{4s}$ laminate is selected for the predictions of FWE method.

It is seen from Figure 2 that the prediction of FWE for the $[0/90]_{4s}$ laminate is very close to the prediction of Ertas and Sonmez,[15] and the curve provides an approximate prediction compared to the experimental data until 10^5 cycles lifetime, and after that it slightly underestimates the data. However, FTPF and SB slightly overestimates the data until 10^5 cycles with the same predictions, and after that point they make close prediction. As seen in Figure 3, the FWE prediction for the $[0/45/-45/90]_{2s}$ is very close to the prediction of Ertas and Sonmez[15] and in a good agreement with the experimental data. However, FTPF and SB predictions slightly underestimate the data at first, and then overestimate the data towards the end with close predictions to each other.

Carbon/epoxy composite laminates. Fatigue life predictions for $[0/90_2]_s$, $[0/90_4]_s$ and $[0_2/90_2]_s$ carbon/epoxy laminates[23] under tension–tension fatigue testing ($R = 0.1$) are shown in Figures 4 to 6, respectively. It should be noted that $[\pm45]_{2s}$ carbon/epoxy laminate is selected as the reference curve for the predictions using FWE and ST models.

For the $[0/90_2]_s$ laminate, it is seen from Figure 4 that the prediction of ST is in better agreement with the experimental data than the predictions of FTPF, SB and FWE models. For the $[0/90_4]_s$, $[0_2/90_2]_s$ laminates (Figures 5 and 6), FWE and ST predict in a wider range of stress amplitude according to the data. It can be said that ST predicts the fatigue behavior with a more average accuracy. However, FTPF and SB make the same underestimated predictions for all the laminates.

E-glass/epoxy composite laminates. In Figures 7 to 9, fatigue life predictions for $[0/90/90/0]_s$, $[45/0/0/-45]_s$ and $[45/90/-45/0]_s$ E- glass/epoxy laminates[24] under zero-tension fatigue testing ($R = 0$) are presented, respectively. It can be noted that $[45/-45/-45/45]_s$ laminate of the same material is selected as the reference curve for the predictions of FWE and ST models.

It is seen from Figure 7 that the predictions of the FTPF and SB models for the $[0/90/90/0]_s$ laminate are identical and in a very good agreement with the experimental data. Nevertheless, FWE model underestimates the experimental data to a degree. On the other hand, ST model slightly overestimates the data. As seen in Figure 8, prediction curve of ST model fits the

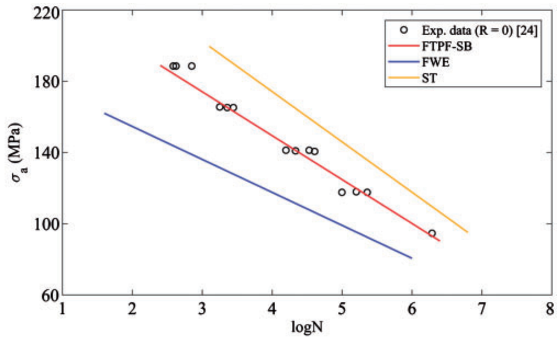

Figure 7. Fatigue life predictions for $[0/90/90/0]_s$ E-glass/epoxy laminate.

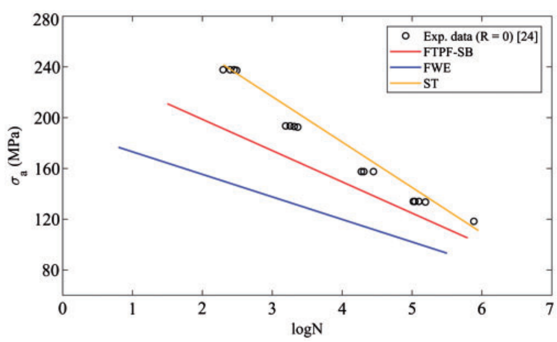

Figure 8. Fatigue life predictions for $[45/0/0/-45]_s$ E-glass/epoxy laminate.

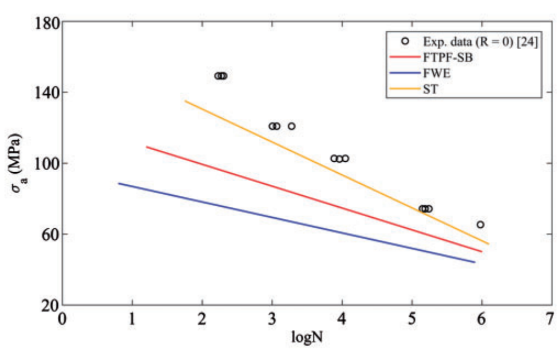

Figure 9. Fatigue life predictions for $[45/90/-45/0]_s$ E-glass/epoxy laminate.

experimental data very well for the $[45/0/0/-45]_s$ laminate. However, FTPF and SB slightly underestimates the data with the identical predictions, and FWE further underestimates the data. It can be seen in Figure 9 that ST model prediction curve is in a good agreement with the data; however, the prediction curves of FTPF-SB and FWE models underestimate the data in increasing degrees, respectively.

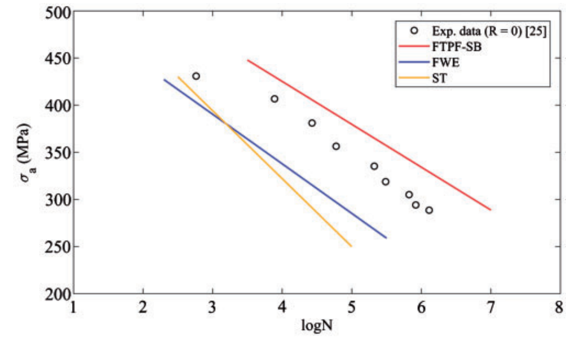

Figure 10. Fatigue life predictions for $[0/90]_{4s}$ carbon/PEEK laminate.

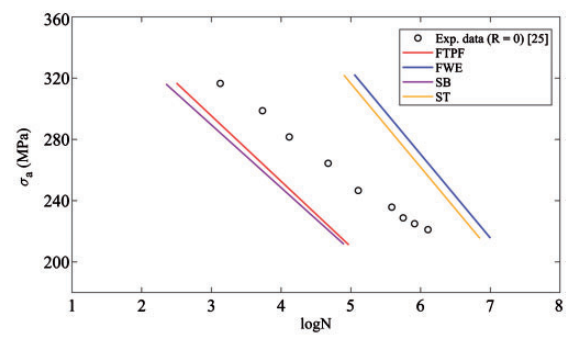

Figure 11. Fatigue life predictions for $[0/45/90/-45]_{2s}$ carbon/PEEK laminate.

Carbon/PEEK composite laminates. Fatigue life predictions for $[0/90]_{4s}$ and $[0/45/90/-45]_{2s}$ carbon/PEEK[25] laminates under zero-tension fatigue testing ($R=0$) are shown in Figures 10 and 11, respectively. For the $[0/90]_{4s}$, $[30]_{16}$ and $[60]_{16}$ laminate curves and for the $[0/45/90/-45]_{2s}$ laminate, $[15]_{16}$ and $[\pm 45]_{4s}$ laminate curves are selected as reference curves for the predictions of FWE and ST models, respectively.

It is seen for the $[0/90]_{4s}$ laminate that the models generally make close predictions. However, FTPF and SB models slightly overestimate the experimental data with identical predictions. FWE and ST underestimate the data to some degree with close prediction curves. For the $[0/45/90/-45]_{2s}$ laminate, FWE and ST overestimate between the life of 10^5 and 10^7 cycles with close prediction curves. On the other hand, FTPF and SB slightly underestimate the data with close prediction curves.

Regarding all the results, the estimation study indicates that any fatigue life prediction model is not obviously better than the other in simulating fatigue life behavior of the composite laminates. Besides, it seems that FTPF and SB models have more prone to predict the fatigue behavior in all the multidirectional laminates of different composite material compared to the other models. ST model shows a better performance in carbon/epoxy and glass/epoxy laminates. FWE model makes the best prediction in graphite/epoxy laminates. In carbon/PEEK laminates, all the models show tendency to underestimate or overestimate the experimental data.

Optimization

The second part of the study is the optimization of composite laminates for different design cases using the fatigue life prediction models and a hybrid algorithm. The hybrid algorithm is constituted by MATLAB Optimization Toolbox.[26] Generalized pattern search algorithm (GPSA) is hybridized with particle swarm algorithm (PSA).

Hybrid algorithm

Hybrid methods combining two different metaheuristic optimization algorithms have been used by the researchers in the literature to take advantages of each powerful side of these algorithms.[17,27–29] For this purpose, first, the initial algorithm is applied to obtain a point close to the global minimum, and then the other selected algorithm is applied to refine and improve the result obtained by the initial algorithm; thus, the possibility of global convergence is increased to a significant degree depending on the nature of the problem. Accordingly, in this study, the combination of GPSA and PSA is considered as the hybrid algorithm to achieve a high accuracy rate in our results. The initial algorithm is PSA, and the GPSA runs after the PSA terminates for each iteration. In the following sections, brief information about each algorithm is given.

GPSA is a derivative-free optimization method developed by Torczon[30] for unconstrained optimization of functions and later extended to cover nonlinear constrained optimization problems. As opposed to the traditional local optimization methods that use information about the gradient or partial derivatives to search for an optimal solution, GPSA is a direct search method which finds a sequence of points x_i that approach the global optimal point through many iterations. Each iteration consists of two phases: the search phase and the poll phase. In the search phase, the objective function is evaluated at a finite number of points on a mesh to find a new point with a lower objective function value than the best current solution. In the poll phase, the objective function is evaluated at the neighboring mesh points to see if a lower objective function value can be obtained.[31]

PSA is on the other hand a population-based algorithm. In this respect, it is similar to the genetic algorithm. A collection of individuals called particles move in steps throughout a region. At each step, the algorithm evaluates the objective function at each particle. After this evaluation, the algorithm decides on the new velocity of each particle. As the particles move, the algorithm reevaluates. The inspiration for the algorithm is flocks of birds or insects swarming. Each particle is attracted to some degree to the best location it has found so far, and also to the best location any member of the swarm has found. After several steps, the population can coalesce around one location if the algorithm finds the global, or can coalesce around a few locations if the algorithm finds local optima, or can continue to move if there is a better solution.[32]

The optimization procedure which describes how PSA works and interacts with GPSA in the hybrid algorithm is given in Figure 12 and explained step by step as follows:

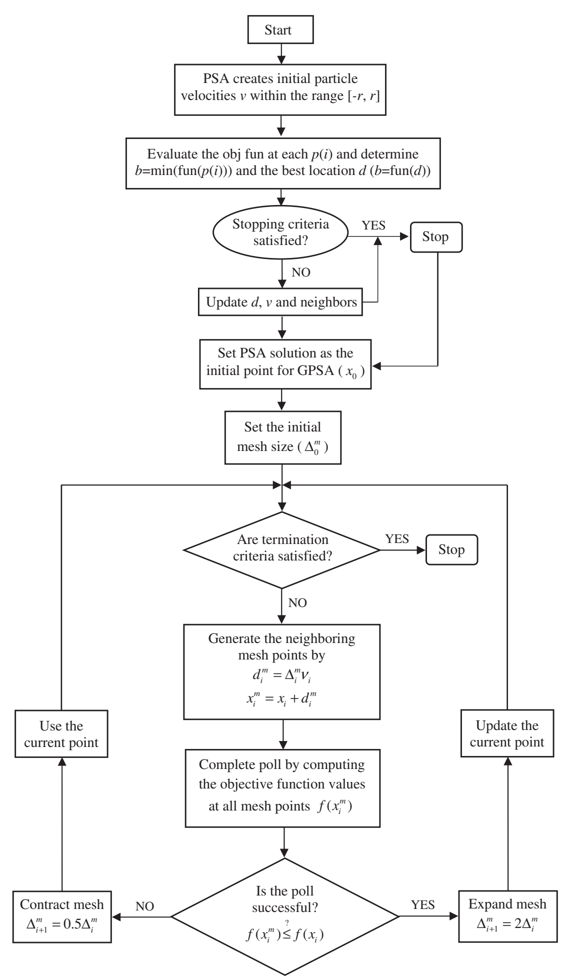

Figure 12. Flowchart of the hybrid PSA-GPSA optimization. PSA-GPSA: particle swarm algorithm-generalized pattern search algorithm.

Step 1. PSA begins by creating the initial particles and assigning them initial velocities v uniformly within the range $[-r, r]$, where r is the vector of initial ranges.

Step 2. It evaluates the objective function at each particle location p(i) of each particle i, and determines the best (lowest) function value $b = \min(\text{fun}(p(i)))$ and the best location d.

Step 3. It chooses new velocities based on the current velocity, the particles' individual best locations, and the best locations of their neighbors.

Step 4. It then iteratively updates the particle locations (the new location is the old one plus the velocity, modified to keep particles within bounds), velocities, and neighbors.

Step 5. Iterations proceed until the algorithm reaches a stopping criterion.

Step 6. When the PSA terminates, the reached optimal solution is used as an initial point for GPSA to search.

Step 7. GPSA starts its search with the initial solution x_0 and an initial mesh size Δ_0^m.

Step 8. If the search phase satisfies a solution with a lower objective function value than the best current solution, the algorithm stops.

Step 9. If termination criteria not satisfied, the algorithm goes to the poll phase and generates a set of neighboring mesh points x_i^m by multiplying the current mesh size by each pattern vector $\{d_i\}$. The fixed-direction pattern vectors are used to determine the points to search at each iteration and defined by the independent variables in the objective function, commonly the maximal basis with $2N$ vectors consisting of N positive and N negative vectors, and the minimal basis with $N+1$ vectors.

Step 10. In the polling step at kth iteration, GPSA polls all the mesh points by computing their objective function values $f(x_i^m)$ in order to find an improved point.

Step 11. If the poll is successful, which means an improved point is found, the current mesh size is multiplied as $\Delta_{i+1}^m = 2\Delta_i^m$, and the current point is updated by the new mesh size for the next iteration $k+1$. If the polling fails to find an improved point, the mesh size is reduced by $\Delta_{i+1}^m = 0.5\Delta_i^m$, and this current point is used for the next iteration.

This process continues through many iterations until global optimum is reached.

There is not any other study except the Deveci and Artem[17] in the literature on fatigue life modeling and/or optimization study by hybridization of meta-heuristic algorithms. In this regard, the proposed hybrid PSA-GPSA algorithm brings a new approach to the solution of optimization problems for fatigue life advance of laminated composites.

Algorithm performance

A buckling optimization problem previously studied[33,34] is considered as a test problem and solved with the selected options to evaluate the performance of the hybrid PSA-GPSA algorithm in terms of computer processor time (CPU time) and maximization of critical buckling load factor with the best stacking sequences. The results of the hybrid algorithm are compared with the best-known results studied by different hybrid algorithms in the literature.[35–38] Table 1 shows the details of composite plate dimensions a and b, and in-plane loads N_{xx} and N_{yy} for the load cases.

The optimum critical buckling load factors for all the load cases are compiled from the literature and presented together with the present critical buckling load factor, stacking sequence and CPU time results in Table 2. The best results are given for load cases 1–4 in the table.

In the table, the critical buckling load factor (λ_{cb}) results are given in British units to provide consistency with the literature. CPU times are average of the best cases specified in each load case and given in seconds [s]. Ply contiguity constraint for stacking sequences is applied to the first three load cases. Besides, stacking sequences are subjected to symmetry and balance constraints. In order to provide an average quality of solutions, each load case is performed 100 times with different starting points.

It can be seen from the table that the present λ_{cb} values for the test problem are found superior to the results given in the literature for load cases 1, 2 and 3. It should be noted that λ_{cb}^{17} represents the results of the previous published study of the authors obtained from the hybrid algorithm combining genetic algorithm (GA) and GPSA, and the present proposed PSA-GPSA algorithm finds greater λ_{cb} values in much shorter CPU time than the GA-GPSA hybrid algorithm. In load case 4, the same results are obtained

Table 1. Load cases for test problem.

Load case	Number of plies	a (mm)	b (mm)	N_{xx} (N/mm)	N_{yy} (N/mm)
1	48	508	127	17.5	2.2
2	48	508	127	17.5	4.4
3	48	508	127	17.5	8.8
4	64	508	254	17.5	17.5

Table 2. Performance results of the hybrid PSA-GPSA algorithm.

Load Case	λ_{cb}^{35-38} ([lbf/in^3]/[lbf/in^3])	λ_{cb}^{17} ([lbf/in^3]/[lbf/in^3])	CPU time[17] [s]	$\lambda_{cb}^{present}$ ([lbf/in^3]/[lbf/in^3])	CPU time^{present} [s]	Stacking sequence ^{present}
1	16120.38	20950.55	372.44	22385.40	106.02	$[90_4/\pm45]_{4s}$
	16119.48	20920.39		22303.53		$[(90_4/\pm45)_3/\pm45/90_2/\pm45]_s$
	16087.83	20894.53		22273.37		$[(90_4/\pm45)_3/\pm45_3]_s$
2	13442.04	15961.75	376.25	16769.66	97.59	$[(90_4/\pm45)_3/90_2/\pm45/90_2]_s$
	13441.28	15729.07		16766.43		$[(90_4/\pm45)_3/90_2/\pm45_2]_s$
	13435.94	15512.55		16727.65		$[(90_4/\pm45)_3/\pm45/90_2/\pm45]_s$
3	10003.53	10591.61	376.12	11192.70	95.82	$[90_4/\pm45]_{4s}$
	10002.95	10460.19		11151.77		$[(90_4/\pm45)_3/\pm45/90_2/\pm45]_s$
	9999.45	10343.85		11136.69		$[(90_4/\pm45)_3/\pm45_3]_s$
4	3973.01[a]	3973.01	439.94	3973.01	314.75	$[\pm45/90_{10}/(\pm45/90_8)_2]_s$
	3973.00[a]	3973.00		3973.00		$[90_4/(90_2/\pm45)_3/90_8/\pm45/90_6]_s$

[a]The optimum values calculated from the stacking sequences of the references.
PSA-GPSA: particle swarm algorithm-generalized pattern search algorithm.

for the first and second optima in a shorter CPU time. λ_{cb} values denoted with superscript a are the real optimum values calculated from the stacking sequence designs given by the related references. It can be noted that λ_{cb} values found[35–38] are possibly misrepresented due to round of error in their optimization procedures. This test study implies that the proposed PSA-GPSA hybrid algorithm shows very good performance in searching the design space within a short time for laminated composite optimization and has capability to yield the best possible results for the fatigue optimization studies.

Fatigue life maximization using the models

Validation of the proposed fatigue optimization strategy

In the optimization part of the study, multidirectional laminate derivations are produced to increase the fatigue life theoretically using different fatigue life prediction models and the PSA-GPSA hybrid algorithm. It is obvious that the optimum stacking sequences giving maximum fatigue lives require a validation supporting the proposed fatigue optimization strategy. In this regard, a pre-optimization study is performed to justify the theoretical derivation procedure using experimental data from the literature. The prediction and optimization procedures are applied to different multidirectional composite laminates.[22,24,25] For each laminate, first, estimated fatigue life is determined. Then, the optimum laminate configurations to be replaced with the tested laminate are investigated and the stacking sequences with increased fatigue lives are obtained. The results are presented in Table 3 with the stacking sequences and experimental fatigue lives of the reference materials. In the table, the maximized results for each case are shown and the corresponding fatigue lives are given as logarithmic.

It is seen in Table 3 that the predicted fatigue life values obtained by each one of the models show differences compared to the experimental fatigue life values. In general, the FTPF, FWE and ST models can make good predictions in different proximities for almost all the stacking sequences (e.g. $[0/90/90/0]_s$[24], $[0/90]_{4s}$[22] and $[0/90]_{4s}$[25]). However, life predictions of the FWE model are typically lower than the other models (e.g., $[45/90/-45/0]_s$[24] and $[0/90]_{4s}$[25]). It can also be noted that the ST method is not capable of predicting for the stacking sequences[22] since the cyclic stress ratio R is -1.

The optimization results show that longer fatigue lives can be obtained with mostly same stacking sequences of the laminates; however, fatigue life values show differences according to the model. For example, while a fatigue life of 10^5 cycles level is reached experimentally and predictively for the $[45/90/-45/0]_s$ sequence[24] for each model, different fatigue lives are achieved by the same optimum $[0/45/90/0]_s$ sequence. ST model yields the optimum sequences with longer fatigue lives not less but more than 10^8 cycles when compared with the other models.

Considering that the fatigue lives of the laminates[22,24,25] are mostly predicted with an acceptable accuracy by all the models, and the optimum stacking sequences having longer fatigue lives than the experimental and predicted lives are obtained by the optimization, it can be concluded that the optimum results obtained theoretically will be acceptable.

Optimization problems and results

In this optimization study, the aim is to investigate the optimum fiber stacking sequences of the laminated composites for maximum fatigue life using FTPF,

Table 3. Fatigue life prediction and optimization using different models for various experimental data.

Stacking sequence	Experimental fatigue life	Model	Predicted fatigue life	Optimized stacking sequence	Maximized fatigue life
$[0/90/90/0]_s$[24]	6.2871	FTPF	6.2500	$[0/90/0/0]_s$	7.5434
		FWE	5.4519	$[0/90/0/0]_s$	6.9816
		SB	6.2500	$[0/90/0/0]_s$	6.8270
		ST	6.8149	$[0/90/0/0]_s$	9.1027
$[45/0/0/-45]_s$[24]	5.8845	FTPF	5.2760	$[0/0/45/0]_s$	6.0207
		FWE	4.5529	$[0/0/45/0]_s$	6.4233
		SB	5.2760	$[0/0/45/0]_s$	6.4812
		ST	5.7986	$[0/0/45/0]_s$	8.2089
$[45/90/-45/0]_s$[24]	5.9772	FTPF	5.1948	$[0/45/90/0]_s$	7.4445
		FWE	4.0734	$[0/45/90/0]_s$	7.6495
		SB	5.1948	$[0/45/90/0]_s$	7.2081
		ST	5.7200	$[0/45/90/0]_s$	10.2409
$[0/90]_{4s}$[22]	6.1121	FTPF	6.4412	$[0_3/90]_{2s}$	6.1402
		FWE	5.2487	$[0_3/90]_{2s}$	6.1343
		SB	6.4412	$[0_3/90]_{2s}$	5.7544
		ST	–[a]	–[a]	–[a]
$[0/\pm45/90]_{2s}$[22]	6.3413	FTPF	7.0128	$[0/90/(0_2/45)_2]_s$	7.5819
		FWE	5.8453	$[(0/45)_2/0_3/90]_s$	6.5744
		SB	7.0129	$[0/90/(0_2/45)_2]_s$	6.5139
		ST	–[a]	–[a]	–[a]
$[0/45/90/-45]_{2s}$[25]	6.1058	FTPF	4.6015	$[0/45/0/90]_{2s}$	10.8758
		FWE	6.8997	$[0_3/45/0_3/90]_s$	6.4986
		SB	4.5257	$[0/45/0/90]_{2s}$	7.6704
		ST	6.7481	$[0/45/0/90]_{2s}$	9.9679
$[0/90]_{4s}$[25]	6.1125	FTPF	6.9716	$[0/(0/90)_3/0]_s$	10.5854
		FWE	5.0038	$[0_3/90]_{2s}$	6.7503
		SB	6.9716	$[0/(0/90)_3/0]_s$	10.7224
		ST	4.5741	$[0_3/90]_{2s}$	10.3122

[a]Method cannot make a feasible prediction or does not yield any feasible optimum solution.
FTPF: Failure tensor polynomial in fatigue; FWE: Fawaz–Ellyin; SB: Sims–Brogdon; ST: Shokrieh–Taheri.

Table 4. Properties of the laminates used in the study.[7]

Material properties	Strength properties	Fatigue properties
$E_{11} = 54.72$ GPa	$X_t = -X_c = 1235.64$ MPa	$X = 1387.62 - 135.92 \log N$
$E_{22} = 17.75$ GPa	$Y_t = -Y_c = 41.19$ MPa	$Y = 39.38 - 2.23 \log N$
$G_{12} = 6.01$ GPa	$S_{21} = 82.38$ MPa	$S = 75.54 - 7.02 \log N$
$\nu_{12} = 0.285$		

FWE, SB, and ST fatigue life prediction models and is thus to determine the potential usability of the models on future fatigue design applications by evaluating the feasibility of the results. Therefore, the stacking sequence of the laminate and fatigue life N is determined for each design case in the optimization. The number of distinct laminae n and the thickness of the laminae t_0 of the laminates are predefined in the design. The orientation angles are considered as the discrete values of 0°, 45°, −45°, 90° which are conventional in industry. The composite material used in this study is taken from the study of Hashin and Rotem.[7] The laminated composite material is a unidirectional 32-layer E-glass/epoxy. The ply thickness t_0 is 0.250 mm. Stress ratio R is 0.1 and frequency ν is 19 Hz. The material, strength and fatigue properties are presented in Table 4.

We have considered several problems including in-plane cyclic loadings N_{xx}, N_{yy}, N_{xy} (load per unit length) applied in combinations of tension, compression and shear loads. The PSA-GPSA hybrid algorithm is used to solve the optimization problems.

The laminates are subjected to symmetry and balance geometric constraints to avoid undesirable stiffness coupling effects. Apart from that, in order to decrease the probability of large scale matrix cracking and to provide damage tolerant structures,[33] ply contiguity constraint is applied to the laminates by constraining the maximum number of contiguous plies of the same orientation to four.

Consequently, the optimization problem can be defined as

Maximize: $\log N(\theta_k)$, $\theta_k \in \{0_2, \pm 45, 90_2\}$, $k = 1, \ldots, 32$

Models: FTPF, FWE, SB, ST
Constraints: Symmetry
Balance
Ply contiguity
Tool: MATLAB Optimization Toolbox

where the number of design variables θ_k decreases to 8 from 32 due to balanced and symmetric configuration of the plates. Hence, composite plates are to be arranged in the sequence of $[\pm\theta_1/\pm\theta_2/\pm\theta_3/\pm\theta_4/\pm$

Table 5. Optimum stacking sequence designs and the corresponding fatigue lives for various in-plane tension cyclic loads.

Loading	Model	Stacking sequence	Global optima	Fatigue life
4/0/0	FTPF	$[(0_4/90_2)_2/0_2/90_2]_s$	21(5)	1.177×10^8
	FWE	$[0_2/\pm45/(0_4/\pm45)_2]_s$	23(5)	3.345×10^8
	SB	$[(0_4/90_2)_2/0_2/90_2]_s$	20(3)	1.318×10^8
	ST	$[0_2/\pm45/(0_4/\pm45)_2]_s$	40(6)	3.211×10^7
4/1/0	FTPF	$[(0_4/\pm45)_2/\pm45/0_2]_s$	16(3)	4.356×10^8
	FWE	$[\pm45/0_2]_{4s}$	13(6)	9.693×10^6
	SB	$[\pm45/(0_4/\pm45)_2/0_2]_s$	21(1)	2.867×10^8
	ST	$[(0_4/\pm45)_2/\pm45/0_2]_s$	50(7)	4.939×10^5
4/2/0	FTPF	$[0_2/(0_2/\pm45)_2/0_4/\pm45]_s$	20(3)	1.353×10^9
	FWE	$[\pm45_5/0_2/\pm45_2]_s$	1(1)	3.229×10^5
	SB	$[(0_4/\pm45)_2/\pm45/0_2]_s$	16(3)	2.267×10^8
	ST	$[(0_4/\pm45)_2/\pm45/0_2]_s$	55(9)	1.617×10^4
4/4/0	FTPF	$[\pm45/0_4/\pm45/90_4/\pm45_2]_s$	67(44)	8.616×10^5
	FWE	$[0_2/90_2]_{4s}$	48(20)	3379
	SB	$[\pm45/0_4/\pm45/90_4/\pm45_2]_s$	76(57)	1.699×10^5
	ST	–[a]	–[a]	–[a]
4/6/0	FTPF	$[\pm45_4/(90_2/\pm45)_2]_s$	13(13)	1061
	FWE	–[a]	–[a]	–[a]
	SB	–[a]	–[a]	–[a]
	ST	–[a]	–[a]	–[a]
6/0/0	FTPF	$[0_2/\pm45/(0_4/\pm45)_2]_s$	22(3)	7.685×10^5
	FWE	$[0_2/\pm45/(0_4/\pm45)_2]_s$	23(4)	2.956×10^7
	SB	$[0_2/\pm45/(0_4/\pm45)_2]_s$	33(6)	6.563×10^5
	ST	$[(0_4/\pm45)_2/0_2/\pm45]_s$	32(5)	1.474×10^4
6/2/0	FTPF	$[(0_4/\pm45)_2/\pm45/0_2]_s$	13(2)	2.695×10^6
	FWE	$[\pm45_3/(0_2/\pm45)_2/0_2]_s$	8(7)	2.542×10^4
	SB	$[(0_4/\pm45)_2/\pm45/0_2]_s$	33(5)	8.502×10^5
	ST	–[a]	–[a]	–[a]
6/3/0	FTPF	$[0_4/(\pm45/0_2/\pm45)_2]_s$	23(9)	7.414×10^4
	FWE	$[(\pm45_2/0_2)_2/\pm45_2]_s$	6(6)	1054
	SB	$[0_4/(\pm45/0_2/\pm45)_2]_s$	20(8)	1.729×10^4
	ST	–[a]	–[a]	–[a]
8/0/0	FTPF	$[(0_4/\pm45)_2/\pm45/0_2]_s$	22(4)	9277
	FWE	$[(0_2/\pm45)_2/0_4/\pm45/0_2]_s$	20(3)	2.538×10^6
	SB	$[(0_4/\pm45)_2/\pm45/0_2]_s$	35(4)	7295
	ST	–[a]	–[a]	–[a]
8/2/0	FTPF	$[0_2/\pm45/0_4/(\pm45/0_2)_2]_s$	26(6)	7690
	FWE	$[0_2/\pm45/(\pm45/0_2)_3]_s$	14(9)	2043
	SB	$[0_2/\pm45/0_4/(\pm45/0_2)_2]_s$	15(2)	2847
	ST	–[a]	–[a]	–[a]

[a]The model yields unfeasible designs in which fatigue lives are smaller than 10^3 cycles.
FTPF: Failure tensor polynomial in fatigue; FWE: Fawaz–Ellyin; SB: Sims–Brogdon; ST: Shokrieh–Taheri.

$\theta_5/\pm\theta_6/\pm\theta_7/\pm\theta_8]_s$. The fiber angles are used as ply stacks of 0_2, ±45, 90_2 for the design cases. MATLAB Optimization Toolbox[26] is used to constitute the hybrid PSA embedded GPSA with predefined operators.

Regarding the optimization strategy, in order to determine the fatigue life of a laminate, first, fatigue life of each lamina is calculated using the equations of each model which are induced to log N formulations and then the

Table 6. Optimum stacking sequence designs and the corresponding fatigue lives for various in-plane tension-compression cyclic loads.

Loading	Model	Stacking sequence	Global optima	Fatigue life
1/−4/0	FTPF	$[90_2/(90_2/0_2/90_2)_2/0_2]_s$	13(3)	1.495×10^8
	FWE	$[90_4/\pm45/90_4/0_2/\pm45/90_2]_s$	18(1)	6.647×10^5
	SB	$[90_2/(90_2/0_2/90_2)_2/0_2]_s$	32(6)	3.017×10^8
	ST	$[(0_4/90_2)_2/0_2/90_2]_s$	36(7)	3.533×10^{32}
1/−6/0	FTPF	$[90_2/\pm45/90_4/(\pm45/90_2)_2]_s$	37(4)	9.281×10^4
	FWE	$[90_4/\pm45/90_4/0_2/\pm45/90_2]_s$	21(2)	1684
	SB	$[90_2/\pm45/90_4/(\pm45/90_2)_2]_s$	36(5)	8.962×10^4
	ST	$[0_2/90_2]_{4s}$	47(17)	8.917×10^{30}
1/−8/0	FTPF	$[90_4/(\pm45/90_2)_3]_s$	31(5)	1855
	FWE	–[a]	–[a]	–[a]
	SB	$[90_4/(\pm45/90_2)_3]_s$	28(3)	1705
	ST	$[0_4/(90_4/0_2)_2]_s$	44(16)	2.074×10^{27}
2/−2/0	FTPF	$[(0_2/90_2)_2/90_2/0_4/90_2]_s$	48(17)	3.153×10^9
	FWE	$[(0_2/90_2)_2/90_2/0_4/90_2]_s$	50(29)	1.185×10^8
	SB	$[(0_2/90_2)_2/90_2/0_4/90_2]_s$	45(14)	2.844×10^9
	ST	$[(0_2/\pm45)_2/0_4/\pm45/0_2]_s$	16(2)	8.331×10^{26}
2/−4/0	FTPF	$[(90_4/0_2)_2/0_2/90_2]_s$	7(2)	1.662×10^8
	FWE	$[(90_4/0_2)_2/90_2/\pm45]_s$	25(3)	8.901×10^5
	SB	$[(90_4/0_2)_2/0_2/90_2]_s$	39(7)	4.792×10^8
	ST	$[0_2/(0_2/\pm45_2)_2/\pm45]_s$	12(10)	2.036×10^{22}
2/−6/0	FTPF	$[(\pm45/90_4)_2/0_2/90_2]_s$	51(5)	3.238×10^4
	FWE	$[90_4/\pm45/90_4/0_2/\pm45/90_2]_s$	21(2)	3010
	SB	$[90_4/(0_2/90_2)_2/\pm45/90_2]_s$	36(5)	6.278×10^4
	ST	$[\pm45_3/0_4/\pm45_3]_s$	25(25)	8.775×10^{18}
4/−2/0	FTPF	$[(0_4/90_2)_2/0_2/90_2]_s$	37(8)	1.662×10^8
	FWE	$[0_4/90_4/0_4/\pm45/0_2]_s$	34(8)	8.901×10^5
	SB	$[(0_4/90_2)_2/0_2/90_2]_s$	36(6)	4.792×10^8
	ST	$[0_2/\pm45/(0_4/\pm45)_2]_s$	30(5)	1.241×10^{13}
4/−4/0	FTPF	$[(0_2/90_2)_2/(90_2/0_2)_2]_s$	50(18)	2.075×10^7
	FWE	$[(0_2/90_2)_2/(90_2/0_2)_2]_s$	49(23)	2.437×10^5
	SB	$[(0_2/90_2)_2/(90_2/0_2)_2]_s$	43(19)	1.098×10^8
	ST	$[(0_4/\pm45)_2/\pm45/0_2]_s$	20(5)	1.637×10^{21}
4/−6/0	FTPF	$[(90_4/0_2)_2/0_2/90_2]_s$	39(6)	4.153×10^4
	FWE	$[(90_4/0_2)_2/0_2/90_2]_s$	37(5)	4145
	SB	$[(90_4/0_2)_2/0_2/90_2]_s$	35(8)	2.188×10^5
	ST	$[\pm45/0_2]_{4s}$	53(26)	1.036×10^{19}
6/−2/0	FTPF	$[(0_4/\pm45)_2/90_2/0_2]_s$	22(5)	3.238×10^4
	FWE	$[\pm45]_{8s}$	1(1)	1.323×10^4
	SB	$[0_2/90_2/0_2/\pm45/0_4/90_2/0_2]_s$	28(1)	6.278×10^4
	ST	$[0_2/(0_2/\pm45)_3/0_2]_s$	39(9)	2.797×10^7
6/−4/0	FTPF	$[0_2/(0_2/90_2)_3/0_2]_s$	37(9)	4.153×10^4
	FWE	$[0_2/(0_2/90_2)_3/0_2]_s$	42(6)	4145
	SB	$[0_2/(0_2/90_2)_3/0_2]_s$	43(8)	2.188×10^5
	ST	$[0_2/\pm45/(0_4/\pm45)_2]_s$	32(5)	9.460×10^{12}
6/−6/0	FTPF	–[a]	–[a]	–[a]
	FWE	–[a]	–[a]	–[a]
	SB	$[0_2/90_2]_{4s}$	46(15)	6361
	ST	$[(0_4/\pm45)_2/\pm45/0_2]_s$	18(3)	7.512×10^{17}

[a]The model yields unfeasible designs in which fatigue lives are smaller than 10^3 cycles.

FTPF: Failure tensor polynomial in fatigue; FWE: Fawaz–Ellyin; SB: Sims–Brogdon; ST: Shokrieh–Taheri.

minimum value among the obtained fatigue lives is chosen as the fatigue life of the laminate. This selection additionally guarantees the first-ply fatigue failure strength. In the optimization, a laminate configuration is accepted to be more fatigue-resistant than other configurations providing that the fatigue life found by the fatigue model is longer than the fatigue lives of the others.

In order to increase the efficiency and reliability of the algorithm, at least 100 independent searches are performed for each case. Different load levels and combinations which allow feasible designs are investigated. The optimum stacking sequences of laminates, the fatigue lives in cycles, and the number of global optima found for various in-plane cyclic loads ($N_{xx}/N_{yy}/N_{xy}$) obtained using the four different models are presented in Tables 5 to 8. Since multiple global optima exist in many loading cases, only one stacking sequence is shown for each loading in the tables. For the global optima in the tables, values outside brackets denote the number of global optima, and values inside brackets

Table 7. Optimum stacking sequence designs and the corresponding fatigue lives for various in-plane tension and shear cyclic loads.

Loading	Model	Stacking sequence	Global optima	Fatigue life
0/2/2	FTPF	$[(\pm45/90_2)_3/\pm45_2]_s$	39(31)	1.598×10^7
	FWE	–[a]	–[a]	–[a]
	SB	$[\pm45/90_2/\pm45_2]_{2s}$	19(19)	1.871×10^7
	ST	$[(0_2/90_4)_2/0_2/90_2]_s$	12(2)	3.854×10^{26}
0/4/2	FTPF	$[\pm45/90_2/(90_2/\pm45)_3]_s$	21(15)	4.747×10^4
	FWE	–[a]	–[a]	–[a]
	SB	$[\pm45/90_2/(90_2/\pm45)_3]_s$	22(15)	7.102×10^4
	ST	$[90_2/(0_2/90_4)_2/0_2]_s$	9(2)	7.572×10^{20}
0/0/4	FTPF	$[\pm45]_{8s}$	1(1)	2.075×10^7
	FWE	–[a]	–[a]	–[a]
	SB	$[\pm45]_{8s}$	1(1)	1.098×10^8
	ST	$[\pm45]_{8s}$	1(1)	1.402×10^6
0/2/4	FTPF	$[\pm45_2/90_2/\pm45_5]_s$	8(8)	2919
	FWE	–[a]	–[a]	–[a]
	SB	$[\pm45_2/90_2/\pm45_5]_s$	8(8)	7485
	ST	$[(0_2/90_4)_2/0_2/90_2]_s$	9(2)	3.854×10^{26}
2/0/2	FTPF	$[0_2/(0_2/\pm45_2)_2/\pm45]_s$	24(17)	1.598×10^7
	FWE	$[\pm45_2/(0_2/\pm45_2)_2]_s$	7(7)	4.730×10^4
	SB	$[\pm45_2/(0_2/\pm45_2)_2]_s$	19(18)	1.871×10^7
	ST	$[(0_4/90_2)_2/0_2/90_2]_s$	27(6)	7.063×10^9
2/2/2	FTPF	$[\pm45]_{8s}$	1(1)	7.180×10^6
	FWE	$[(90_4/0_2)_2/0_2/90_2]_s$	11(2)	1361
	SB	$[\pm45]_{8s}$	1(1)	7.866×10^6
	ST	$[0_4/90_4/0_4/90_2/0_2]_s$	25(2)	1.673×10^8
2/4/2	FTPF	$[(\pm45_2/90_2)_2/\pm45_2]_s$	13(12)	1588
	FWE	–[b]	–[b]	–[b]
	SB	$[(\pm45_2/90_2)_2/\pm45_2]_s$	16(15)	1500
	ST	$[0_2/90_2/(0_4/90_2)_2]_s$	40(6)	7.358×10^6
4/2/1	FTPF	$[0_2/\pm45_2/0_4/\pm45_3]_s$	14(10)	7.746×10^5
	FWE	$[0_4/90_4/0_4/90_2/0_2]_s$	23(5)	1.986×10^4
	SB	$[0_2/\pm45_2/0_4/\pm45_3]_s$	20(18)	4.704×10^5
	ST	$[0_4/90_4/0_4/90_2/0_2]_s$	29(4)	1948
4/0/2	FTPF	$[\pm45_2/0_4/(\pm45/0_2)_2]_s$	22(12)	4.747×10^4
	FWE	$[0_2/(0_2/90_2)_2/0_4/90_2]_s$	24(4)	8721
	SB	$[\pm45_2/0_4/(\pm45/0_2)_2]_s$	23(9)	7.102×10^4
	ST	$[0_2/(0_2/90_2)_2/0_4/90_2]_s$	28(4)	1.388×10^4
4/2/2	FTPF	$[(0_2/\pm45)_2/\pm45_4]_s$	17(16)	1588
	FWE	$[90_2/(0_4/90_2)_2/0_2]_s$	24(3)	2482
	SB	$[(0_2/\pm45)_2/\pm45_4]_s$	16(15)	1500
	ST	$[90_2/(0_4/90_2)_2/0_2]_s$	27(5)	1948

[a]The model does not give any solution by the optimization.
[b]The model yields unfeasible designs in which fatigue lives are smaller than 10^3 cycles.
FTPF: Failure tensor polynomial in fatigue; FWE: Fawaz–Ellyin; SB: Sims–Brogdon; ST: Shokrieh–Taheri.

Table 8. Optimum stacking sequence designs and the corresponding fatigue lives for various in-plane tension-compression-shear cyclic loads.

Loading	Model	Stacking sequence	Global optima	Fatigue life
1/−1/1	FTPF	$[\pm45_4/(0_2/90_2)_2]_s$	74(70)	3.766×10^8
	FWE	$[\pm45_4/90_2/0_2/90_2/\pm45]_s$	18(17)	3.406×10^7
	SB	$[\pm45_4/(0_2/90_2)_2]_s$	84(77)	4.166×10^8
	ST	$[0_4/(90_2/0_2)_3]_s$	28(5)	3.828×10^{17}
1/−2/1	FTPF	$[(90_4/\pm45)_2/90_2/0_2]_s$	55(6)	7.434×10^7
	FWE	$[(\pm45/90_2)_2/90_2/0_2/\pm45_2]_s$	28(22)	1.127×10^7
	SB	$[(90_4/\pm45)_2/90_2/0_2]_s$	65(12)	8.780×10^7
	ST	$[0_2/(0_2/90_2)_3/0_2]_s$	24(1)	1.899×10^{20}
1/−4/1	FTPF	$[90_4/\pm45_2/90_4/0_2/90_2]_s$	44(6)	1.542×10^6
	FWE	$[90_4/\pm45/90_4/0_2/90_2/\pm45]_s$	21(2)	2.267×10^5
	SB	$[90_4/\pm45_2/90_4/0_2/90_2]_s$	40(7)	1.811×10^6
	ST	$[(0_4/90_2)_2/0_2/90_2]_s$	39(7)	3.533×10^{32}
1/−1/2	FTPF	$[\pm45_3/0_2/\pm45_3/90_2]_s$	39(39)	1.533×10^7
	FWE	$[\pm45_5/0_2/\pm45_2]_s$	1(1)	3.588×10^5
	SB	$[\pm45_3/0_2/\pm45_3/90_2]_s$	38(38)	1.810×10^7
	ST	$[0_2/(0_2/90_2)_2/0_4/90_2]_s$	28(4)	3.828×10^{17}
1/−2/2	FTPF	$[(\pm45_2/90_2)_2/\pm45/90_2]_s$	12(8)	3.138×10^6
	FWE	$[\pm45_2/90_2/\pm45_2/0_2/\pm45_2]_s$	7(7)	2.743×10^5
	SB	$[(\pm45_2/90_2)_2/\pm45/90_2]_s$	15(12)	4.171×10^6
	ST	$[(0_4/90_2)_2/0_2/90_2]_s$	27(5)	1.899×10^{20}
1/−4/2	FTPF	$[(90_4/\pm45)_2/\pm45/90_2]_s$	13(3)	6.534×10^4
	FWE	$[\pm45_3/90_4/0_2/\pm45/90_2]_s$	21(15)	5419
	SB	$[(90_4/\pm45)_2/\pm45/90_2]_s$	29(5)	1.049×10^5
	ST	$[0_2/90_2/(0_4/90_2)_2]_s$	14(3)	3.533×10^{32}
2/−2/1	FTPF	$[(90_2/0_2)_3/\pm45_2]_s$	75(49)	1.533×10^7
	FWE	$[(90_2/0_2)_3/\pm45_2]_s$	69(46)	9.328×10^6
	SB	$[(90_2/0_4)_2/90_2/\pm45]_s$	83(40)	1.819×10^7
	ST	$[(0_2/\pm45)_2/0_4/\pm45/0_2]_s$	13(1)	2.303×10^{13}
2/−4/1	FTPF	$[90_4/\pm45/90_4/0_4/90_2]_s$	38(8)	5.144×10^5
	FWE	$[(90_4/0_2)_2/90_2/\pm45]_s$	28(3)	3.864×10^5
	SB	$[90_4/\pm45/90_4/0_4/90_2]_s$	52(8)	6.321×10^5
	ST	$[0_2/90_2/(0_4/90_2)_2]_s$	31(4)	3.730×10^{14}
2/−6/1	FTPF	$[0_2/(90_4/\pm45)_2/90_2]_s$	43(6)	4566
	FWE	$[90_4/\pm45/90_4/0_2/90_2/\pm45]_s$	21(2)	2402
	SB	$[90_4/\pm45/90_4/0_2/90_2/\pm45]_s$	47(9)	7716
	ST	$[0_2/90_2/(0_4/90_2)_2]_s$	31(4)	4.032×10^{18}
4/−4/1	FTPF	$[(0_2/90_2)_2/(90_2/0_2)_2]_s$	48(13)	1.040×10^5
	FWE	$[(0_2/90_2)_2/(90_2/0_2)_2]_s$	28(9)	1.342×10^5
	SB	$[(0_2/90_2)_2/(90_2/0_2)_2]_s$	45(15)	2.212×10^5
	ST	$[(0_4/\pm45)_2/\pm45/0_2]_s$	16(3)	1.740×10^{13}
2/−2/2	FTPF	$[\pm45/90_2/0_2/\pm45/0_2/90_2/\pm45_2]_s$	79(75)	6.725×10^5
	FWE	$[\pm45_3/90_4/0_2/\pm45_2]_s$	18(17)	3.469×10^5
	SB	$[\pm45/90_2/0_2/\pm45/0_2/90_2/\pm45_2]_s$	78(74)	9.738×10^5
	ST	$[0_2/(0_2/90_2)_3/0_2]_s$	27(6)	7.521×10^{11}
2/−4/2	FTPF	$[(\pm45/90_2)_2/90_2/0_2/90_2/\pm45]_s$	71(27)	1.272×10^4
	FWE	$[(\pm45/90_2)_2/90_2/0_2/90_2/\pm45]_s$	26(11)	7.376×10^4
	SB	$[90_2/(90_2/\pm45/90_2)_2/0_2]_s$	56(9)	1.913×10^4
	ST	$[(90_2/0_4)_2/90_2/0_2]_s$	31(3)	3.730×10^{14}

FTPF: Failure tensor polynomial in fatigue; FWE: Fawaz–Ellyin; SB: Sims–Brogdon; ST: Shokrieh–Taheri.

denote the number of optimum stacking sequences ensuring the ply contiguity constraint. The optimum results with fatigue lives smaller than 10^3 cycles are not included in the tables.

Table 5 shows the results for only tension cyclic loads. As the results indicate, the fatigue life is found to be sensitive to the level of stress. For each N_{xx} loading level, 4, 6 and 8 ($\times 10^2$ N/mm), fatigue lives of the optimum designs generally decrease with the increase of N_{yy} loading as may be expected. However, fatigue lives of the designs show increase for 4/0/0–4/1/0–4/2/0 and 6/0/0–6/2/0 loading increments in the optimization with FTPF and SB models. Moreover, fatigue life range varies according to the model. Maximum range and values of fatigue lives are mostly obtained by the FTPF. Optimum fatigue-resistant designs can be achieved for almost all the design cases by the FTPF, FWE and SB model optimizations. Nevertheless, ST model does not yield any feasible optimum design for 4/4/0, 4/6/0, 6/2/0, 6/3/0, 8/0/0 and 8/2/0 loading cases. Besides, the models except FTPF do not give feasible designs for 4/6/0 loading. It can also be noted that the same optimum designs are obtained with different fatigue life values by the models (e.g. 4/0/0 and 6/0/0).

Table 6 shows the results for tension-compression cyclic loads. Optimum stacking sequences with reasonable fatigue lives ranging between 10^3 and 10^9 cycles can be obtained by FTPF, FWE and SB models according to the given loadings. However, ST model finds optimum designs having excessive fatigue lives for all the given loadings, which is unrealistic considering the loading magnitudes and the results of the other models. FTPF and SB models provide designs with much higher fatigue life than FWE. It is also noted that identical stacking sequences can be obtained by the FTPF, FWE and SB models for specific loadings.

Table 7 shows the results for different tension and shear cyclic loads. The same optimum stacking sequences can be obtained by the models for specific loading cases. Optimum stacking sequences with reasonable fatigue lives ranging between 10^3 and 10^8 cycles can be obtained by all the models according to the given loadings. However, ST model finds optimum designs having excessive fatigue lives in the 0/2/2, 0/4/2 and 0/2/4 zero-tension-shear type loadings. FTPF and SB models yield designs with fatigue life in the same cycle-level for many loadings (e.g., 2/0/2 and 4/2/1), and ST can find comparable results with FTPF and SB such as in 4/0/2 loading. On the other hand, it seems that FWE can achieve to obtain optimum designs with a lower fatigue life compared to the other models for 2/0/2, 2/2/2, 4/2/1, 4/0/2 loadings, whereas it cannot find any optimum solution for 0/2/2, 0/4/2, 0/2/4 zero-tension-shear and 0/0/4 pure shear cyclic loadings. It is also seen that the presence of shear load significantly decreases the maximized fatigue life. For example, while fatigue life can be maximized to 1.353×10^9 in the 4/2/0 loading for the FTPF, the fatigue lives in 4/2/1 and 4/2/2 loading cases are obtained as 7.746×10^5 and 1588, respectively.

Table 8 shows the results for several tension-compression-shear cyclic loading cases. It is seen that maximum fatigue life of the designs decreases as the compression and shear loads are increased. Optimum stacking sequences with feasible fatigue lives ranging between 10^3 and 10^8 cycles are obtained by FTPF, FWE and SB models according to the given loadings. FTPF and SB yield the same stacking sequences with fatigue lives that can be close to each other in the optimization. However, FWE yields designs with lower fatigue life compared to FTPF and SB in many loading cases (e.g. 1/−4/1, 1/−1/2, and1/−4/2), and optimization by ST model yields stacking sequences with very high fatigue lives, which is unrealistic.

It is typically seen in the optimization that FTPF and SB models yield acceptable stacking sequence designs with proper fatigue life values. However, the optimization with FWE model generally gives designs with lower fatigue life compared to the FTPF and SB, and even gives no design for zero-tension-shear loading type. Also, overestimated fatigue-resistant designs are obtained by the optimization with ST model, which is impractical considering the maximized life values of the other models. This situation may arise from two reasons. First, FWE and ST are very sensitive to the selection of reference S–N curve and the chosen reference curve may not be accurate for the models. Second, the usage of ST model for the prediction is limited to unidirectional composite laminate under tension–tension and compression–compression loading cases. This limitation seems also valid for the optimization with ST model considering the designs having overestimated fatigue lives.

Conclusion

In this study, the estimation and optimization capabilities of the fatigue life prediction models, FTPF, FWE, SB and ST on multidirectional composite laminates are investigated for comparison.

For the estimation part, fatigue life predictions of multidirectional graphite/epoxy, glass/epoxy, carbon/epoxy and carbon/PEEK composites in different laminate configurations taken from the literature are obtained. It is seen that the models can simulate the fatigue behavior of various multidirectional composite laminates of different materials in different approximations. Any model has no obvious advantage over the other models. However, FTPF and SB are more prone to make estimations that could be acceptable in all the laminates. Besides, while FTPF and SB models mostly make the same estimations, FWE and ST makes different estimations compared to them. These variable prediction results lead to the necessity to research the optimal design capability of the models.

In the optimization part of the study, a hybrid algorithm composed of PSA and GPSA is used as search algorithm. A buckling optimization problem with different design cases is selected as a test problem and solved to evaluate the performance of the hybrid algorithm. The results are compared with the published data in the literature. It is seen that the PSA-GPSA hybrid algorithm has the capability to find better results in a shorter time than the other algorithms compared. After the reliability of the algorithm is ensured, the fatigue optimization strategy is also validated for all the models through comparisons of their prediction and fatigue life maximization results with the experimental data that belong to different composite materials and multidirectional laminate configurations from the literature.

Finally, a number of fatigue optimization problems that include stacking sequence design cases for various in-plane cyclic loadings are solved using the FTPF, FWE, SB and ST models. The results of the optimization study for maximum fatigue life imply that FTPF and SB models produce more reliable fatigue-resistant designs than FWE and ST models considering that the fatigue life values reached by the ST are irrationally high in many cases, and FWE yields less number of reliable designs than the others. Hence, it can be concluded that FTPF and SB are more reasonable to use in optimization compared to FWE and ST. This situation possibly arises from that FTPF and SB use the S–N curve equations of [0], [±45] and [90] laminates to constitute their models, which guarantees a more robust mechanical model. However, the FWE and ST models use only one S–N curve equation to constitute their models, and these off-axis S–N curves should be selected wisely as they directly affect the accuracy of the predictions. In this respect, it is also understood that even if fatigue life prediction models with one reference S–N curve give accurate fatigue life predictions, this does not mean that they will give feasible optimum stacking sequence results.

As a concluding remark, this study makes a unique contribution to the literature as it addresses both the fatigue life prediction of multidirectional laminates of different composite materials and the optimization for fatigue-resistant stacking sequence designs by using different models. In this regard, the study reveals the abilities of the chosen models in terms of modeling and improvement of fatigue life of laminated composites for potential use by engineers and designers.

Declaration of conflicting interests

The author(s) declared no potential conflicts of interest with respect to the research, authorship, and/or publication of this article.

Funding

The author(s) received no financial support for the research, authorship, and/or publication of this article.

References

1. Vassilopoulos AP and Keller T. *Fatigue of fiber-reinforced composites*. London, UK: Springer-Verlag, 2011.
2. Quaresimin M, Susmel L and Taljera R. Fatigue behaviour and life assessment of composite laminates under multiaxial loadings. *Int J Fatigue* 2010; 32: 2–16.
3. Liu Y and Mahadevan S. A unified multiaxial fatigue damage model for isotropic and anisotropic materials. *Int J Fatigue* 2007; 29: 347–359.
4. Kennedy CR, Bradaigh CM and Leen SB. A multiaxial fatigue damage model for fibre reinforced polymer composites. *Compos Struct* 2013; 106: 201–210.
5. Dong H, Li Z, Wang J, et al. A new fatigue failure theory for multidirectional fiber-reinforced composite laminates with arbitrary stacking sequence. *Int J Fatigue* 2016; 87: 294–300.
6. Hashin Z and Rotem A. A fatigue failure criterion for fiber reinforced materials. *J Compos Mater* 1973; 7: 448–464.
7. Rotem A. Fatigue failure of multidirectional laminate. *AIAA J* 1979; 17: 271–277.
8. Sims DF and Brogdon VH. Fatigue behavior of composites under different loading modes. In: Reifsnider KL and Lauraitis KN (eds) *Fatigue of filamentary materials*. ASTM STP 636, American Society for Testing and Materials, 1977, pp.185–205.
9. Fawaz Z and Ellyin F. Fatigue failure model for fibre-reinforced materials under general loading conditions. *J Compos Mater* 1994; 28: 1432–1451.
10. Philippidis TP and Vassilopoulos AP. Fatigue strength prediction under multiaxial stress. *J Compos Mater* 1999; 33: 1578–1599.
11. Kawai M. A phenomenological model for off-axis fatigue behavior of unidirectional polymer matrix composites under different stress ratios. *Compos Part A Appl S* 2004; 35: 955–963.
12. Shokrieh MM and Taheri-Behrooz F. A unified fatigue life model based on energy method. *Compos Struct* 2006; 75: 444–450.
13. Adali S. Optimisation of fiber reinforced composite laminates subject to fatigue loading. *Compos Struct* 1985; 3: 43–55.
14. Walker M. A method for optimally designing laminated plates subject to fatigue loads for minimum weight using a cumulative damage constraint. *Compos Struct* 2000; 48: 213–218.
15. Ertas AH and Sonmez FO. Design optimization of fiber-reinforced laminates for maximum fatigue life. *J Compos Mater* 2014; 48: 2493–2503.
16. Muc A and Muc-Wierzgoń M. Discrete optimization of composite structures under fatigue constraints. *Compos Struct* 2015; 133: 834–839.

17. Deveci HA and Artem HS. Optimum design of fatigue-resistant composite laminates using hybrid algorithm. *Compos Struct* 2017; 168: 178–188.
18. Vassilopoulos AP. *Fatigue life prediction of composites and composite structures*. Cambridge, UK: Woodhead Publishing Limited, 2010.
19. Tsai SW and Hahn HT. *Introduction to composite materials*. Lancaster: Technomic, 1980.
20. Sandhu RS, Gallo RL and Sendeckyj GP. In initiation and accumulation of damage in composite laminates. In: Daniel IM (ed) *Composite Materials: Testing and Design* (Sixth Conference). ASTM STP 787, American Society for Testing and Materials, 1982, pp. 163–182.
21. El Kadi H and Ellyin F. Effect of stress ratio on the fatigue failure of fiberglass reinforced epoxy laminae. *Composites* 1994; 25: 917–924.
22. Rotem A and Nelson HG. Residual strength of composite laminates subjected to tensile-compressive fatigue loading. *J Compos Technol Res* 1990; 12: 76–84.
23. Naderi M and Maligno AR. Fatigue life prediction of carbon/epoxy laminates by stochastic numerical simulation. *Compos Struct* 2012; 94: 1052–1059.
24. Lian W and Yao W. Fatigue life prediction of composite laminates by FEA simulation method. *Int J Fatigue* 2010; 32: 123–133.
25. Jen MHR and Lee CH. Strength and life in thermoplastic composite laminates under static and fatigue loads. Part I: experimental. *Int J Fatigue* 1998; 20: 605–615.
26. Optimization Toolbox™. *MATLAB computer software in version R2016b*. Natick, Massachusetts, USA: The Mathworks, Inc., 2016.
27. Yogeswaran M, Ponnambalam SG and Tiwari MK. An efficient hybrid evolutionary heuristic using genetic algorithm and simulated annealing algorithm to solve machine loading problem in FMS. *Int J Prod Res* 2009; 47: 5421–5448.
28. Alarifi A, Liu Z, Erenay FS, et al. Dynamic optimization of lurgi type methanol reactor using hybrid GA-GPS algorithm: the optimal shell temperature trajectory and carbon dioxide utilization. *Ind Eng Chem Res* 2016; 55: 1164–1173.
29. Deveci HA, Aydin L and Artem HS. Buckling optimization of composite laminates using a hybrid algorithm under Puck failure criterion constraint. *J Reinf Plast Compos* 2016; 35: 1233–1247.
30. Torczon V. On the convergence of pattern search algorithms. *SIAM J Optim* 1997; 7: 1–25.
31. Nicosia G and Stracquadanio G. Generalized pattern search algorithm for peptide structure prediction. *Biophys J* 2008; 95: 4988–4999.
32. MATLAB. *Global optimization toolbox user's guide, MATLAB computer software in version R2016b*. Natick, Massachusetts, USA: The Mathworks, Inc., 2016, pp.384–395.
33. Riche RL and Haftka RT. Optimization of laminate stacking sequence for buckling load maximization by genetic algorithm. *AIAA J* 1993; 31: 951–956.
34. Soremekun G, Gürdal Z, Haftka RT, et al. Composite laminate design optimization by genetic algorithm with generalized elitist selection. *Comput Struct* 2001; 79: 131–143.
35. Rao ARM and Arvind N. A scatter search algorithm for stacking sequence optimisation of laminate composites. *Compos Struct* 2005; 70: 383–402.
36. Rao ARM and Arvind N. Optimal stacking sequence design of laminate composite structures using Tabu embedded simulated annealing. *Struct Eng Mech* 2007; 25: 239–268.
37. Rao ARM and Lakshmi K. Optimal design of stiffened laminate composite cylinder using a hybrid SFL algorithm. *J Compos Mater* 2012; 46: 3031–3055.
38. Rao ARM. Lay-up sequence design of laminate composite plates and a cylindrical skirt using ant colony optimization. *Proc IMechE Part G: J Aerospace Eng* 2009; 223: 1–18.